ELSEVIER

Chemical Engineering Journal 82 (2001) 131–141

Chemical Engineering Journal

www.elsevier.com/locate/cej

Influence of the ejector configuration, scale and the gas density on the mass transfer characteristics of gas–liquid ejectors

P.H.M.R. Cramers [a,b], A.A.C.M. Beenackers [a,*]

[a] *Department of Chemical Engineering, University of Groningen, 9747 AG, The Netherlands*

[b] *Kvaerner Process Technology (Switzerland) AG, Buss Industriepark, Hohenrainstrasse 10, CH 4133, Pratteln 1, Switzerland*

Received 18 May 2000; accepted 14 November 2000

Abstract

For the design and scale-up of gas–liquid ejectors, reliable data are required which describe the mass transfer characteristics as a function of the physical fluid properties, geometrical design and the process related parameters. Therefore, the mass transfer characteristics of various ejector geometries and scales were investigated using the desorption of oxygen from water, by means of an inert gas, as a model system. In order to investigate scale-up, the ejector was geometrically scaled-up by a factor of 2 (and hence, a volumetric scale-up by a factor of 8). Since industrial venturi reactors are operated at elevated pressures, the influence of the gas density on the mass transfer characteristics was also studied.

The experimental results show that geometrical design parameters, like the presence of a swirl device in the upstream section of the nozzle, the mixing tube length and the nozzle to mixing tube diameter ratio, all influence the mass transfer characteristics significantly. Further, it was experimentally verified that the gas density influenced the mass transfer characteristics. It was observed that the volumetric mass transfer coefficient ($k_L a$) increases when higher density gases are used.

The main objective of this study is investigating the influence of the ejector geometry on the mass transfer characteristics of gas–liquid ejectors and to formulate design and scale-up rules/criteria.

Keywords: Gas density; Gas–liquid ejectors; Venturi reactors

1. Introduction

Gas–liquid interfacial mass transfer often controls the overall production rate of gas–liquid reactors. High intensity "gas–liquid (in line) mixers", like static mixers, rotor stators and ejectors are increasingly used as a primary gas dispersion device in gas–liquid reactors [1] and Schugerl, 1982. These high intensity mixers can improve the mass transfer rates by generating small bubbles, which are then injected into a reaction vessel/column, thereby improving the mass transfer characteristics of the entire system.

A typical example of such a gas–liquid reactor is the "Loop-Venturi Reactor" (LVR). In this reactor type, the gas phase is initially dispersed in the venturi (ejector) section. Recently, these venturi reactors have frequently been recommended for processes where gas–liquid interfacial mass transfer was the rate-controlling step of the process.

Systematic investigations concerning venturi-reactors have been reported by Cramers et al. [2,3] and Dirix and van de Wiele [4]. According to these authors, it is very important to investigate the mass transfer characteristics of the ejector and reaction vessel separately. Their studies showed that the ejector and the reaction vessel have to be considered as two reactor units in series. The ejector can be modelled as a plug flow reactor, whereas the reaction vessel has to be considered ideally mixed. Experimental verifications showed that the $k_L a$-values of the ejector and the reaction vessel differ by nearly two orders of magnitude.

Although there have been a number of papers on liquid jet ejectors, none of them provides all the information that is required for a reliable design and scale-up as a function of geometrical and process related parameters. To our knowledge there are only three papers in the open literature were the mass transfer characteristics of ejectors have been studied in more detail. The proposed correlation's, which describe the liquid side volumetric mass transfer coefficient of the ejectors used are given in Table 1. This shows that the mass transfer characteristics of ejectors improve when

1. more energy is dissipated per unit mass (ϵ),
2. the gas fraction (higher Q_G/Q_L ratios) is increased.

* Corresponding author. Tel.: +31-50-3634486; fax: +31-50-3634479.
E-mail address: a.a.c.m.beenackers@chem.rug.nl (A.A.C.M. Beenackers).

1385-8947/01/$ – see front matter
PII: S1385-8947(00)00363-6

Nomenclature

a	specific gas–liquid contact area (m^2/m^3)
$C_{1–4}$	empirical constants
C_G	oxygen concentration in the gas phase (mol/l)
C_L	oxygen concentration in the liquid bulk (mol/l)
$C_{L,i}$	oxygen concentration at G/L interface (mol/l)
$C_{L,in}$	oxygen concentration at nozzle entrance (mol/l)
$C_{L,out}$	oxygen concentration at ejector outlet (mol/l)
d_B	bubble diameter (m)
d_D	diffuser diameter (m)
d_M	maximum stable bubble diameter (m)
d_M	mixing tube diameter (m)
d_N	nozzle diameter (m)
d_S	Sauter bubble diameter (m)
D_L	diffusion coefficient in liquid phase (m^2/s)
g	gravitational constant (m/s^2)
He	Henry number ($C_G/C_{L,i}$)
k_L	physical mass transfer coefficient (m/s)
k_La	volumetric mass transfer coefficient (1/s)
(k_La)	volumetric mass transfer coefficient of the ejector (1/s)
$(k_La)^*_{Ej}$	mass transfer number (Eq. (16))
l_s	swirl length (m)
L_D	diffuser length (m)
L_M	mixing tube length (m)
P	power required for gas compression (W)
P_{Jet}	power of discharging jet (W)
$\Delta P_{G,Ej}$	pressure difference of the gas phase across the ejector (Pa)
Q_G	volumetric gas flow rate (m^3/h)
Q_L	volumetric liquid flow rate (m^3/h)
r_N	radius of the nozzle (m)
Sw	swirl number (Eq. (15))
U_{tan}	tangential velocity (m/s)
U_N	jet velocity at the nozzle exit (m/s)
V_{Ej}	effective ejector volume (m^3)

Greek Letters

Θ	swirl angle (rad)
ε_G	gas fraction
$(\varepsilon_G)^*$	gas fraction defined by (Eq. (17))
μ_L	dynamic viscosity (Pa s)
ν_L	kinematic liquid viscosity (m^2/s)
ρ_G	gas density (kg/m^3)
ρ_L	liquid phase density (kg/m^3)
ρ_M	mixture density $= \rho_L$ (1-ε_G) kg/m^3
σ	surface tension (N/m)
ϵ	energy dissipation rate (W/kg)

Further, Dirix and van de Wiele [4] showed that higher k_La-values are obtained when the nozzle to mixing tube diameter ratio is increased. How the other design parameters affect the mass transfer rates has not been reported. Given the variety of ejector configurations studied, it is not surprising that the constants and exponents of the correlations in Table 1 vary considerably.

It should be mentioned that the data of Dirix and van de Wiele [4] were obtained with a spinner (swirl device) in the upstream section of the nozzle, whereas in both other studies, no spinner was present. Whether the presence of this swirl device affects the mass transfer characteristics of the ejector section is still an open question. It is known that the swirl device improves the maximum amount of gas sucked in by ejectors [5]. However, whether the swirl device influences the mass transfer characteristics has not been reported.

The main objective of this study is investigating the influence of the ejector geometry on the mass transfer characteristics of gas–liquid ejectors and to formulate design and scale-up rules/criteria.

2. Development of design relations

In order to develop design relations for the mass transfer characteristics of ejectors, the following theoretical approach is followed. The volumetric mass transfer coefficient (k_La) consists of the physical mass transfer coefficient (k_L) and the specific interfacial area (a).

If a homogeneous gas dispersion is considered, the specific interfacial area follows from

$$a = \frac{6\varepsilon_G}{d_S} \tag{1}$$

The specific interfacial area (a) can be calculated once the gas fraction (ε_G) and Sauter mean bubble diameter (d_S) are known.

Bubble flow is assumed in which small discrete bubbles move downward with nearly the same velocity as the liquid phase, i.e. no slip conditions. Due to the high-energy dissipation rates within ejectors, the bubble sizes dispersed within the ejector section are relatively small. Cramers et al. [2,3] reported averaged bubble sizes in the range between 30 and 60 μm when using a coalescence inhibited medium. When using a coalescence promoting fluid, the averaged bubble sizes were in the range between 0.1 and 1 mm. Therefore, it is justified to assume that the relative velocity difference between the gas and the liquid phase can be neglected. Under these conditions the gas fraction is approximated by

$$\varepsilon_G = \frac{Q_G}{Q_G + Q_L} \tag{2}$$

where Q_L and Q_G are the volumetric liquid and gas flow rates, respectively.

In order to predict d_S, it is assumed that the Sauter bubble diameter can be related to the maximum stable bubble size

Table 1
Correlations for ejector systems from literature

Authors	Correlations	Flow regime
Cramers et al. (1992) [2,3]	$a = 19500\ (\epsilon)^{0.40}\ (1-\varepsilon_G)^{0.40}$	Down flow ejector Non coalescing system
Changfeng et al. (1991) [6]	$k_L a = 0.7206\ (\epsilon)^{0.492}\ (\varepsilon_G)^{0.88}$ $a = 918\ (\epsilon)^{0.372}\ (\varepsilon_G)^{0.261}$ $d_S = 6.52{\cdot}10^{-3}\ (\epsilon)^{-0.372}\ (\varepsilon_G)^{0.261}$	Down flow ejector Coalescing system
Dirix et al. (1990) [4]	(1) $k_L a = 5.4 \times 10^{-3}(\epsilon)^{0.66}\varepsilon_G \left(\frac{d_N}{d_D}\right)^{0.66}$ (2) $k_L a = 8.5 \times 10^{-4}(\epsilon)^{0.66} \left(\frac{d_N}{d_M}\right)^{0.66}$	Down flow ejector Coalescing system (1) Bubble flow regime (2) Jet flow regime

present in a turbulent flow field (d_M). The size distribution of bubbles formed by breaking up in a turbulent flow field has been studied extensively by many workers [7]; Unno and Inoue, 1980; [8] and [9]; Brown and Pitt, 1972; Zang et al., 1985; [10]. These studies show that for coalescing media the ratio between of the Sauter mean bubble and the maximum stable bubble diameter in turbulent pipe flows is constant, i.e.

$$\frac{d_S}{d_M} = \text{constant} = C_1 \tag{3}$$

From the experimental results of the above mentioned studies, it follows that the value of C_1 is nearly constant and varies between 0.6 and 0.7.

Cramers et al. [11] showed that the maximum stable bubble diameter present in a turbulent flow field is approximated by

$$d_M = \left(\frac{We_C}{2}\right)^{0.6} \left(\frac{\sigma^3}{\rho_L^2 \rho_G}\right)^{0.2} (\epsilon)^{-0.4} \left(\frac{1+\varepsilon_G}{1+0.2\varepsilon_G}\right)^{1.2} \tag{4}$$

Substitution of Eqs. (3) and (4) into (1) gives a relation for the specific gas–liquid interfacial area as a function of the gas and liquid physical properties of the liquid phase, the power input per unit mass input and the gas fraction, i.e.

$$a = C_2(\epsilon)^{0.4}\varepsilon_G \left(\frac{1+0.2\varepsilon_G}{1+\varepsilon_G}\right)^{1.2} \tag{5}$$

where

$$C_2 = C_1 \left(\frac{\rho_L^2 \rho_G}{\sigma^3}\right)^{0.2} \left(\frac{We_C}{2}\right)^{-0.6} \tag{6}$$

The physical mass transfer coefficient (k_L) is obtained from the equation of Kawase and Moo-Young [12], i.e.

$$k_L = C_3\sqrt{D_L} \left(\frac{\epsilon}{\nu_L}\right)^{0.25} \tag{7}$$

where D_L and ν_L are the diffusion coefficient of the gas in the liquid and kinematic viscosity, respectively. This equation was obtained from both experimental and theoretical studies. Application of Eq. (7) is most successful for gas–liquid dispersions in which the energy dissipation rate is homogeneously distributed over the entire flow field.

Combination of Eqs. (5) and (7) gives than finally the semi-theoretical relation for $k_L a$

$$k_L a = C_4(\epsilon)^{0.65}\varepsilon_G \left(\frac{1+0.2\varepsilon_G}{1+\varepsilon_G}\right)^{1.2} \tag{8}$$

where

$$C_4 = C_3 \left(\frac{D_L^2}{\nu_L}\right)^{0.25} \left(\frac{\rho_L^2 \rho_G}{\sigma^3}\right)^{0.2} \left(\frac{We_C}{2}\right)^{-0.6}$$

Eq. (8) underlines the importance of the local energy dissipation rate. Therefore, it is essential to define a relation for the energy dissipation rate that is effectively used for gas dispersion.

The energy supplied by a high velocity jet (P_{Jet}) can be expressed as

$$P_{Jet} = 0.5\rho_L U_N^2 Q_L \tag{9}$$

provided, the kinetic energy of the upstream velocity before the nozzle and the downstream velocity of the two phase mixture at the ejector outlet can be neglected. In Eq. (9), U_N equals to the jet velocity at the nozzle exit. The energy supplied by the high velocity jet is mainly used for dispersing the gas phase. However, also a considerable amount of this energy input is used for compressing the gas. In fact, the energy used for gas compression is not effectively used for "mixing" of both phases and should be taken in consideration when calculating the effective energy input by the liquid jet used for gas dispersion. The energy consumed for compressing the gas phase ($P_{Compres}$) can be estimated by

$$P_{Compres} = \Delta P_{G,Ej} Q_G \tag{10}$$

where $\Delta P_{G,EJ}$ equals the gas phase pressure differential across the ejector.

The importance of Eq. (10) is shown in the following example. Cramers et al. [11] has shown that the amount of gas sucked in by the ejector is influenced by the gas phase pressure differential. As an example a jet velocity of 20 m/s and gas- and liquid-flow rates of 5 m^3/h will be assumed. For a Henzler type of ejector, the pressure differential required for obtaining Q_G/Q_L of 1 is approximately 40 kPa. Substitution of these data in Eqs. (9) and (10) shows that under these conditions approximately 20% of the energy supplied by the liquid jet is used for gas compression instead of gas dispersion.

The energy dissipation rate effectively used for gas dispersion (ϵ_{Dis}) can than be calculated as

$$\epsilon_{Dis} = \frac{P_{Jet} - P_{Compres}}{\rho_M V_{Ej}} \quad (11)$$

where ρ_M is the density of the two-phase mixture in the ejector and V_{Ej} the ejector volume. In order to develop design relations for the mass transfer characteristics of ejectors, Eqs. (8) and (11) will be used.

3. Experimental facility and procedures

3.1. Experimental set-up

A schematic diagram of the ejector and the experimental facility used is shown Fig. 5. The volumetric gas–liquid mass transfer rates were calculated from the measured desorption rate of oxygen from the liquid phase (deionised water) into an inert gas phase (when not mentioned the gas phase used is nitrogen) as a model system. The liquid was first aerated in a large supply vessel ($V = 500$ l) before entering the ejector. The temperature and oxygen concentration in the liquid phase were measured continuously at the ejector entrance, ejector outlet and outlet of the reaction vessel (as shown in Fig. 1). The flux of oxygen transferred in the ejector and reaction vessel could, thus, be evaluated separately.

A special measuring cell was developed in which a separation of the gas and the liquid phase was realised. This was necessary to preventing the gas bubbles from interfering with the measurement of the actual oxygen concentration in the liquid phase.

The ejector configuration used in the present study had a mixing tube diameter (d_M) of 12 mm, diffuser outlet diameter of 35 mm (i.e. diffuser angle of approximately 3) and a draft tube length (L_D) of 630 mm. The mixing tube lengths were varied between 24 and 120 mm, respectively. The nozzle diameters used were 4.0, 4.7 and 5.3 mm. Due to confidentiality, the exact geometry and dimensions of the nozzle design and swirl device are not reported. In order to investigate scale-up, the ejector was geometrically enlarged with a factor 2 (the ejector with the mixing tube length of 24 mm).

3.2. Procedures

To gain more insight into the behaviour of venturi reactors, it is necessary to quantify to what extent the mass transfer takes place in the ejector. The decrease of the oxygen concentration in the liquid phase of the ejector can be described by a first order differential equation and a mass balance for oxygen. The following assumptions are made:

- In the ejector, the gas and the liquid move in cocurrent plug flow.
- The gas flow is considered to be constant.

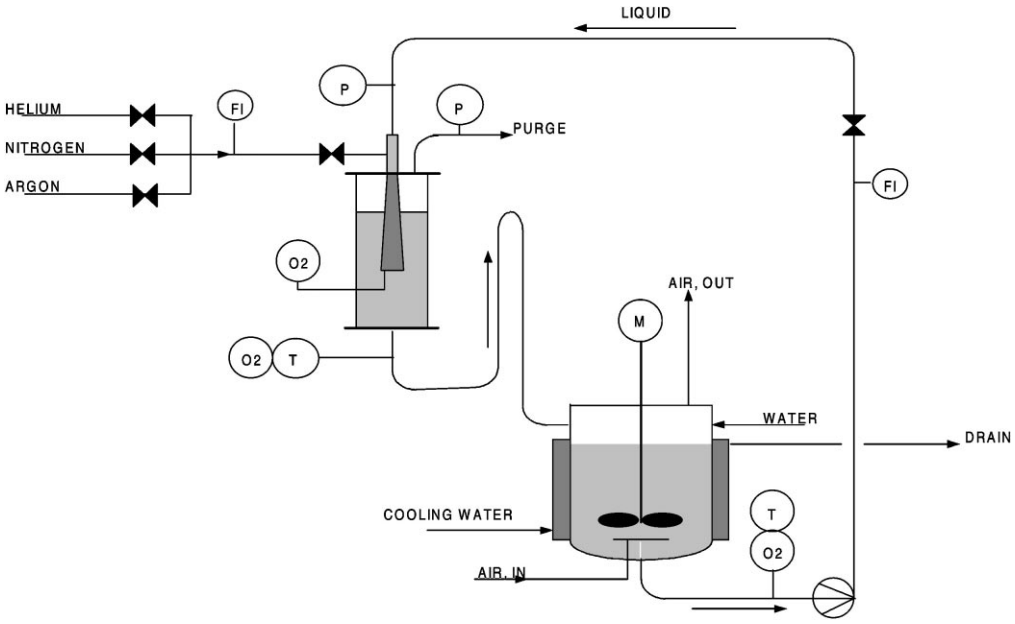

Fig. 1. Scheme of the experimental set-up.

- A pure inert gas is supplied.
- The gas side mass transfer resistance is negligible ($He\ k_G \gg k_L$).

$$Q_L\,dC_L = k_L a(C_{L,i} - C_L)\,dV \tag{12}$$

$$Q_L(C_{L,in} - C_L) = Q_G C_G = Q_G He C_{L,i} \tag{13}$$

The concentration of the oxygen in the liquid phase at the ejector outlet can then be represented by

$$C_{L,out} = C_{L,in}\left(\frac{Q_L/Q_G He + \mathrm{EXP}(-k_L a(V_{Ej}/Q_L)(1+Q_L/Q_G He))}{1+Q_L/Q_G He}\right) \tag{14}$$

where V_{Ej} is the dispersion volume in the ejector and He the Henry coefficient for oxygen in water. Based on molar concentrations and a temperature of 20°C, the Henry-number, $He = 29$.

4. Experimental results

4.1. Hydrodynamics

In this section, the influence of a swirl device in the up-stream section of the nozzle, the d_N/d_M ratio, the mixing tube length and the scale on the ejector hydrodynamics will be discussed.

4.2. Influence of swirl device on flow regime

The experiments have proved that two different flow regimes can be distinguished in ejectors, depending on the gas–liquid flow ratio. At low Q_G/Q_L ratios (and hence, high gas phase pressure differentials) bubbly flow was observed, independent whether a swirl device was present or not. At higher Q_G/Q_L ratios, there was a change in flow regime as illustrated schematically in Fig. 2.

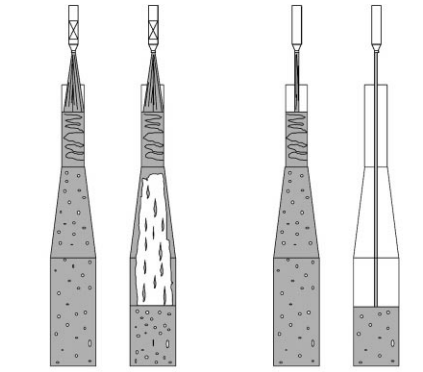

Fig. 2. Flow regimes in the ejector, (a) ejector with swirl device, (b) without swirl device.

In the absence of a swirl device, a slowly widening liquid jet exists which abruptly transforms into a gas–liquid dispersion in the ejector. It was observed that the mixing zone location (the place where the liquid jet discharges into the bubbly mixture) was influenced by the gas–liquid flow ratio, i.e. with increasing gas flow rates (and hence, decreasing $\Delta P_{G,Ej}$) the mixing zone location shifts from the mixing tube entrance towards the ejector outlet. If gas dispersion takes place in the mixing tube, so-called "bubble flow" occurs. If gas dispersion takes place in the diffuser or draft tube, the system operates in the so-called "jet-flow" regime.

When a swirl device was present in the up-stream section of the nozzle, the liquid jet "disintegrated" rather fast, compared to the situation without the swirl device. This fast widening of the liquid jet is caused by the centrifugal forces caused by the tangential velocity component of the swirl. Visually, it was observed that the mixing zone location in the ejector remains nearly fixed in the mixing tube, independent of the gas–liquid flow rate. Although there was no change in the mixing zone location, there was still a change in flow regime. At low gas–liquid flow ratios bubbly flow appeared, with characteristics as observed for bubble flow regime without a swirl device in the nozzle. When using a swirl device, at higher Q_G/Q_L ratios, so-called "jet-annular" flow was observed as illustrated in Fig. 2. In this "jet-annular" flow regime, the gas is dispersed in the mixing tube. At the diffuser wall a "stagnant" liquid layer is formed. The jet in the core of the ejector seemed to consist of a gas stream carrying rags (ligaments) of liquid.

The experimental observations, as described above, have shown that the presence of a swirl device in the nozzle has a significant effect on the ejector hydrodynamics. The influence of the d_N/d_M ratio, the mixing tube length and the scale, on the flow transition point (the Q_G/Q_L flow ratio at which the change in flow regime occurs), is discussed below.

4.3. Influence of geometrical design and scale on flow regime

The influence of the geometrical parameters on the flow transition point are shown in Fig. 3a and b.

Fig. 3a shows that in the absence of a swirl device the flow transition point increases with increasing mixing tube L/D ratio and decreasing d_N/d_M ratio. Further, it can be seen that the transition point is independent of scale.

When a swirl device is present, Fig. 3b shows that the reverse is true. In order to explain this scale effect, the spinning action of the high velocity jet has to be considered. The swirl device in the upstream section of the nozzle gives a tangential velocity component to the liquid flow. The ratio of the tangential to the axial velocity of the jet can be characterised with a swirl number (Sw) [13], which is defined as

$$Sw = \frac{U_{Tan}}{U_{Ax}} = \frac{\Theta r_N}{l_S} \tag{15}$$

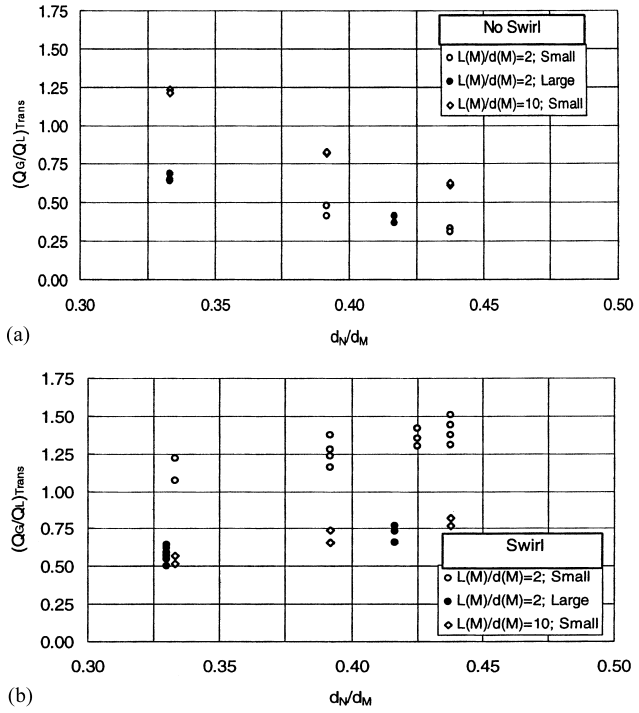

Fig. 3. Influence of the geometrical parameters on flow regimes in the small and enlarged ejector: (a) without swirl device, and (b) ejector with swirl device.

where r_N, Θ and l_s are the nozzle outlet radius and the angle of the spinner and the length of the spinner, respectively. Eq. (15) shows that in a linear scale-up of the swirl device, the tangential velocity of the liquid jet increases (and hence, the swirl number changes), resulting in scale effects. This indicates that for a proper scale-up of an ejector with swirl device in the nozzle, the swirl number has to be kept constant and not the linear dimensions of the swirl device. In other words, a direct linear geometrical scale-up is not possible, since the dimensions of the swirl device have to be adapted.

Since the swirl device causes rotation of the liquid phase, the mixing tube of the ejector can be compared to a hydrocyclone when high swirl numbers are present. With increasing centrifugal forces, separation of the gas and liquid phase is enhanced, resulting in a decrease of the flow transition point and longer mixing tube lengths upon linear scale-up. These centrifugal forces are also responsible for the characteristic "jet-annular" flow regime when applying the swirl device in a nozzle. Due to the rotational forces, both phases will be separated, resulting in a characteristic gas core in both the diffuser and the draft tube section when applying a swirl device in the nozzle.

From the above observations, it is concluded that a direct linear scale-up is only possible when no swirl device is used. When using a swirl device, the geometry of the swirl has to depend on the swirl-number which should be kept constant, to allow a reliable scale-up of the ejector. Since, geometrical parameters affect the local ejector hydrodynamics, it

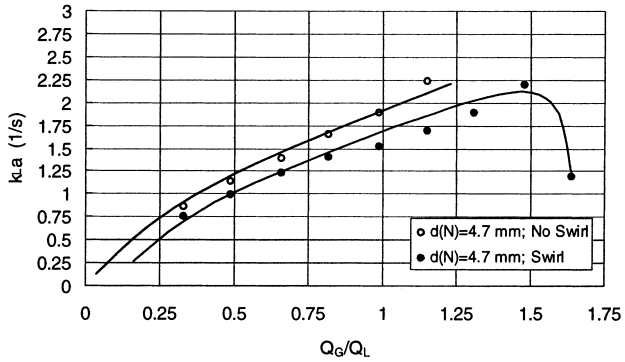

Fig. 4. Influence of a swirl device on the volumetric mass transfer coefficient ($Q_L = 0.5$ l/s, $d_N = 4.7$ mm, $L_M/d_M = 2$, system: water/nitrogen).

is expected that the mass transfer characteristics of ejectors are also influenced by these parameters as will be discussed below.

5. Experimental results

5.1. Mass transfer rates

5.1.1. Influence of the ejector configuration

In the previous section, it has been demonstrated that the ejector configuration has a significant effect on the flow regime in the ejector. Therefore, we investigated the influence of the swirl device, the mixing tube length, d_N/d_M ratio and the effect of scale on the mass transfer performance of ejectors.

5.1.2. Influence of the swirl device

A systematic investigation concerning the influence of a swirl device on k_La has not been reported in the literature yet. Therefore, some preliminary experiments were carried out with an ejector with an L_M/d_M ratio of 2 and a nozzle diameter of 4.7 mm. In Fig. 4, the experimentally determined (k_La)-value is plotted against the volumetric gas/liquid flow ratio. Fig. 5 shows that the ejector without a swirl device creates higher k_La-values compared to the ejector with a swirl device in the nozzle and it is seen that k_La increases with Q_G/Q_L. In the case when a swirl device was present, the two different flow regimes can be clearly distinguished, i.e. the diagram shows a discontinuity at the flow transition point from bubble- to jet-annular flow, respectively. The experimental data as shown in Fig. 4 give a representative example of all the experiments performed.

Since the ejector without a swirl device creates higher k_La-values, it is concluded that this ejector configuration utilises the supplied energy more effectively. In order to verify this statement, the gas phase pressure differential across the ejector ($\Delta P_{G,Ej}$) is plotted versus Q_G/Q_L in Fig. 5. This figure shows that the ejector with swirl device requires higher gas phase pressure differentials for the same Q_G/Q_L.

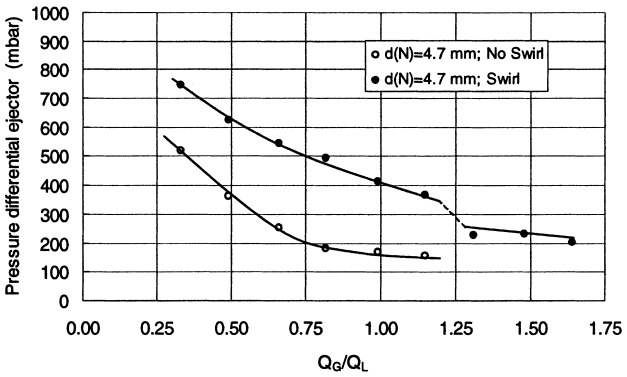

Fig. 5. Influence of the swirl device on the gas phase pressure differential ($Q_L = 0.5$ l/s, $d_N = 4.7$ mm, $L_M/d_M = 2$, system: water/nitrogen).

In other words, when using a swirl device, more energy is used for gas compression instead of gas dispersion.

In order to exclude the effect of the energy consumed for compressing the gas phase, use will made of Eqs. (8) and (11). Therefore, in Fig. 6, $(k_La)^*$ is plotted versus $(\varepsilon_G)^*$ in the ejector. In these figures $(k_La)^*$ and $(\varepsilon_G)^*$ are defined as

$$(k_La)^*_{Ej} = \frac{k_La}{(\epsilon_{Dis})^{0.65}} \tag{16}$$

and

$$(\varepsilon_G)^* = \varepsilon_G \left(\frac{1 + 0.2\varepsilon_G}{1 + \varepsilon_G}\right)^{1.2} \tag{17}$$

Fig. 6 shows that at a constant energy dissipation rate based on ejector volume, ϵ_{Dis}, the ejector without swirl device still creates slightly higher k_La-values.

From this, it can be concluded that a swirl device decreases the efficiency of the ejector with respect to mass transfer. A physical explanation for this observations discussed by Cramers et al. [14].

5.1.3. Influence of the nozzle to mixing tube diameter ratio

Dirix and Van de Wiele [4] have already shown that the ratio between the nozzle to mixing tube diameter (d_N/d_M)

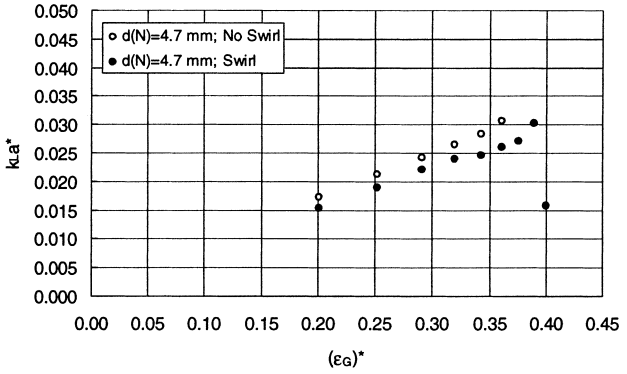

Fig. 6. $(k_La)^*_{Ej}$ vs. $(\varepsilon_G)^*$; $Q_L = 0.5$ l/s; $d_N = 4.7$ mm, $L_M/d_M = 2$ (system: water/nitrogen).

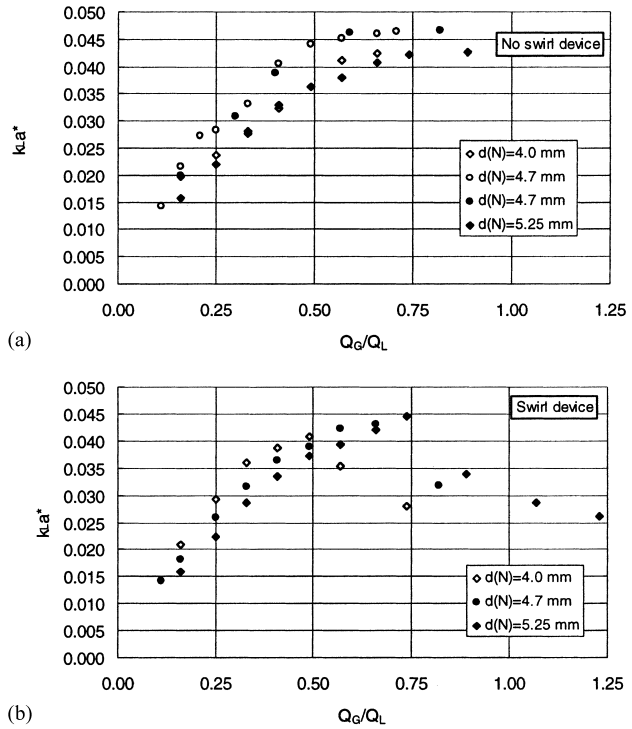

Fig. 7. Influence of the nozzle to mixing tube diameter ratio on $(k_La)^*$. (a) Ejector without swirl device, and (b) ejector with swirl device ($L_M/d_M = 10$ and $d_M = 12$ mm, system: water/nitrogen).

affects the volumetric mass transfer coefficient of ejectors. According to these authors $(k_La) \approx (d_N/d_M)^{0.65}$. The ejector configuration used in their experimental investigation included a swirl device in the upstream section of the nozzle.

Our experimental results of the influence of the nozzle to mixing tube diameter ratio on $(k_La)_{Ej}$ are shown in Fig. 7.

The observations clearly demonstrate that the nozzle diameter, i.e. the d_N/d_M ratio, influences the volumetric mass transfer coefficient of the ejector. However, it can be seen that contradicting effects are observed. When using a swirl device, $(k_La)^*$ decreases when the nozzle diameter is increased. In other words, for a constant power supply to the ejector, the k_La-value is influenced by the geometrical parameters (read the d_N/d_M ratio). When no swirl device is included, it can be seen that there exists an optimum at a d_N/d_M ratio of approximately 0.38.

The data show that $(k_La)^*$ is proportional to and can be correlated by

$$(k_La)^* \approx \left(\frac{d_N}{d_M}\right)^{0.65}, \quad \text{with swirl device} \tag{18}$$

$$(k_La)^* \approx 1 - 0.55\left(0.38 - \frac{d_N}{d_M}\right)^2, \quad \text{without swirl device} \tag{19}$$

as shown in Fig. 8a and b.

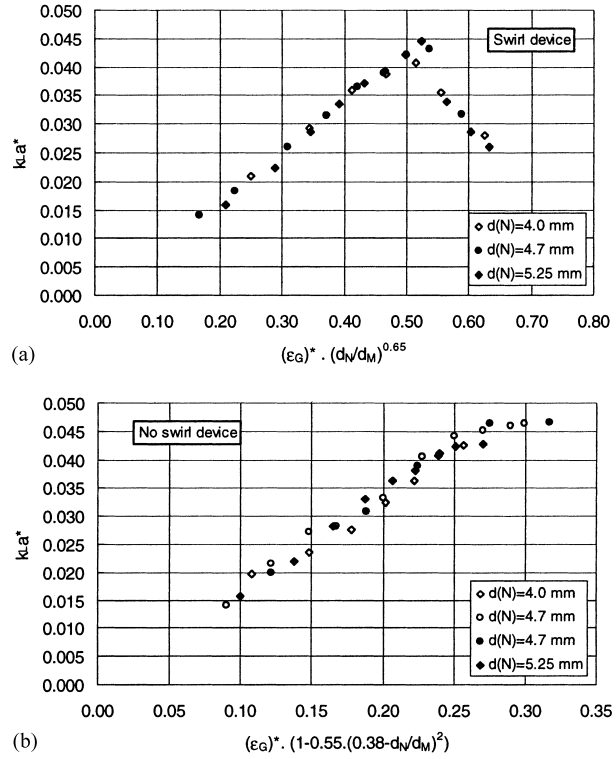

Fig. 8. (a) $(k_La)^*$ vs. $(\varepsilon_G)^*$ $(d_N/d_M)^{0.65}$ (with swirl, $L_M/d_M = 10$ and $d_M = 12$ mm, system: water/nitrogen); (b) $(k_La)^*$ vs. $(\varepsilon_G)^*$ (1–0.55 $(0.38 - d_N/d_M)^2$) (no swirl, $L_M/d_M = 10$ and $d_M = 12$ mm, system: water/nitrogen).

5.1.4. Influence of the mixing tube length

According to the experiments of Dirix and Van de Wiele [4], the mixing tube length has no influence on (k_La). In their study, the mixing tube length to diameter ratio (L_M/d_M) varied between 2 and 10. This observation is in disagreement with our experimental results as shown in Fig. 9.

Further, it can be seen that for all the ejectors studied, $(k_La)^*$ increases linearly with $(\varepsilon_G)^*$ in the bubble flow regime, whereas $(k_La)^*$ decreases linearly with $(\varepsilon_G)^*$ in the so-called jet annular flow regime.

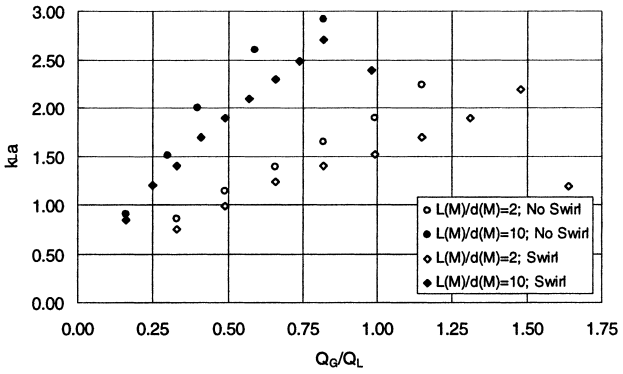

Fig. 9. Influence of the mixing tube length on (k_La) ($Q_L = 0.5$ l/s, $d_N = 4.7$ mm, system: water/nitrogen).

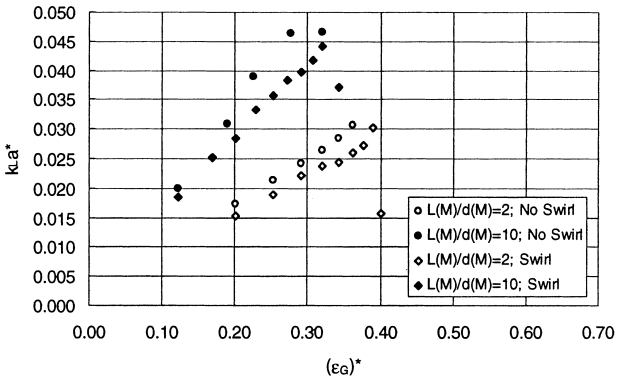

Fig. 10. Influence of the mixing tube length on $(k_La)^*$ ($d_N = 4.7$ mm, system: water/nitrogen).

Fig. 9 clearly illustrates that the ejector with the longer mixing tube creates higher volumetric mass transfer coefficients compared to the ejector with a shorter mixing tube. Also, it is seen that when applying a swirl device, the flow transition point shifts to lower gas–liquid flow ratios for the longer mixing tube. As discussed before, the reverse is true for an ejector without swirl device.

When $(k_La)^*$ is plotted versus $(\varepsilon_G)^*$, four individual curves are obtained, as shown in Fig. 10. This experimental observation indicates that each ejector configuration requires its own specific design correlation. The influence of the mixing tube length on (k_La) can be explained from the local ejector hydrodynamics.

In Fig. 2, a scheme of the local ejector hydrodynamics is shown, which shows the existence of two separate zones in the ejector, i.e. the mixing shock region and bubbly flow in the remaining part of the ejector. In the mixing zone, the dispersion looks “milky”, whereas below this zone a clear bubbly flow is observed. A schematic representation of the hydrodynamics observed is shown in Fig. 11.

For the standard ejector used ($L_M/d_M = 2$), the mixing zone is located in both the mixing tube and in a large volume of the diffuser. However, when the mixing tube length is increased, the mixing zone is nearly completed in the mixing tube. This indicates that the initial dispersion volume (mixing zone volume) is influenced by the ejector configuration. From this visual observation, it is concluded that the mixing zone volume of an ejector with a L_M/d_M ratio of 10 is smaller compared to the mixing zone volume of an ejector with a shorter mixing tube.

Assuming that the major amount of energy is dissipated within the mixing zone, the local energy dissipation rate in the mixing zone (ϵ_{MZ}) can be approximated by

$$\epsilon_{MZ} = \frac{P_{Jet} - P_{Compres}}{\rho_M V_{MZ}} \tag{20}$$

where V_{MZ} equals the mixing zone volume. Eq. (20) shows that the local energy dissipation rate in the ejector with the longer mixing tube is higher, since V_{MZ} is smaller. Since the initial dispersed bubble size is proportional to $(\epsilon_{MZ})^{-0.4}$,

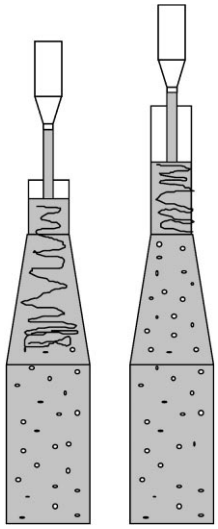

Fig. 11. Influence of the mixing tube length on the ejector hydrodynamics (jet velocity and gas–liquid flow ratio are identical).

Eq. (4), the ejector with the longer mixing tube disperses smaller bubbles and, hence, gives higher k_La-values. From this, it can be concluded that for proper designing and modelling of ejectors, the local hydrodynamics have to be studied in more detail.

5.1.5. Influence of scale

In order to study the influence of scale on the mass transfer performance of ejectors, an ejector with an L_M/d_M ratio of 2 was geometrically enlarged by a factor of 2. An overview of the experiments with these ejectors is shown in Fig. 12.

The results presented in this figure show that the volumetric mass transfer coefficient is independent of the ejector size at the same energy input per unit volume. Also for the ejector without a swirl device no scale effect was found with respect to both k_La and flow transition point. In contrast, for the ejector with a swirl device the flow transition point seemed to be influenced by scale. However, in these experiments the swirl-number was not kept constant during the scale-up procedure. When the ejector is scaled-up properly with respect to the *Sw*-number, this scale dependency will probably vanish [13]. The following scale rules can be derived: for a constant volumetric mass transfer coefficient in the ejector section; equal power-input per unit ejector volume and equal ejector dimensions are required for a proper scale-up of the ejector. These scale rules are valid for all the ejector configurations, whether a swirl device is present in the upstream section of the nozzle or not. However, when using a swirl device, it has to be assured that during scale-up the swirl-number is also kept constant. Otherwise, the flow transition point is affected by scale.

5.1.6. Influence of the gas density on mass transfer characteristics

Recently, it has been recognised that gas density has a significant influence on the mass transfer characteristics of gas–liquid contactors. Studies showed that the mass transfer characteristics of the various gas–liquid reactors improved when higher density gases were used. This effect was attributed to a decrease in the bubble stability when applying higher density gases. Therefore, also an influence of the gas density on (k_La) is to be expected.

In order to illustrate this influence, experiments have been performed with a standard ejector ($L_M/d_M = 2$) with a swirl device in the upstream section of the nozzle. The gases used were helium, nitrogen and argon. The results of these experiments are shown in Fig. 13.

This figure clearly demonstrates that the (k_La)-values in the bubble flow regime are systematically higher when higher density gases are used, whereas in the jet flow regime there seems to be no influence of the gas density on (k_La). The liquid side mass transfer coefficient is not affected by the gas phase used, since oxygen in all cases was desorped from the water phase. Therefore, any change in the (k_La)-value must be due to a change in the specific gas–liquid interfacial area (a).

Cramers et al. [14] demonstrated that the bubble diameter is proportional to $(\rho_G)^{-0.2}$. This indicates that a_{Ej} (and

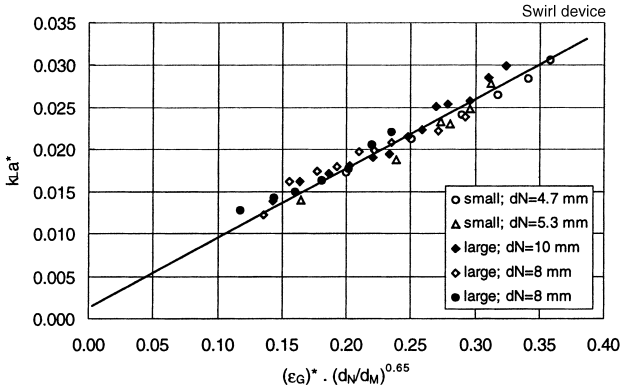

Fig. 12. Overview of experiments performed with the standard ejector and with a device geometrically scaled-up by a factor of 2, both with swirl device in the nozzle ($L_M/d_M = 2$).

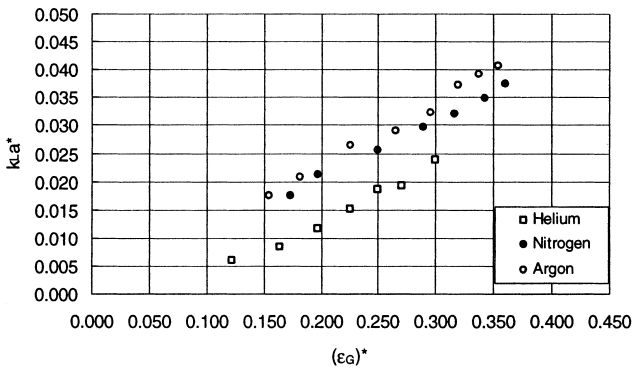

Fig. 13. Influence of the gas density on the volumetric mass transfer coefficient of a standard ejector.

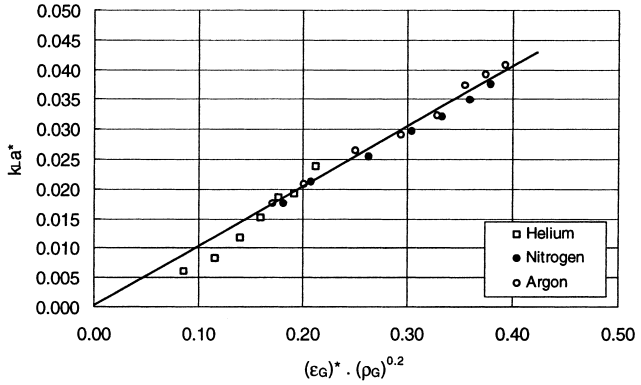

Fig. 14. $(k_La)^*$ vs. $(\varepsilon_G)^*(\rho_G)^{0.2}$; $Q_L = 0.5$ l/s, $d_N = 4.7$ mm, $L_M/d_M = 2$ (swirl device included).

hence, k_La) should be proportional to $(\rho_G)^{-0.2}$. Eq. (8) appears to correlate the experimental data (of the bubble flow regime) very well, see Fig. 14. In this figure $(k_La)^*$ is plotted against $(\varepsilon_G)^*(\rho_G)^{0.2}$.

These results show that Levich's theoretical exponent of 0.2 for the effect of the gas density is in agreement with our experimental observations.

6. Design correlation's

In deriving design relations for the volumetric mass transfer coefficient of ejectors, as a basis Eqs. (8) and (11) have been used

$$k_La = (\epsilon_{Dis})^{0.65}\varepsilon_G\left(\frac{1+0.2\varepsilon_G}{1+\varepsilon_G}\right)^{1.2}\left(\frac{\rho_L^2\rho_G}{\sigma^3}\right)^{0.2} \zeta\left(\frac{d_N}{d_M}\right)\zeta\left(\frac{L_M}{d_M}\right) \quad (22)$$

where $\zeta(d_N/d_M)$ and $\zeta(L_M/d_M)$ include the geometrical effects of the nozzle to mixing tube diameter ratio and the mixing tube length to diameter ratio, respectively.

For the *ejector without swirl device* in the upstream section of the nozzle the data could be correlated as

$$k_La = C_5(\epsilon_{Dis})^{0.65}\varepsilon_G\left(\frac{1+0.2\varepsilon_G}{1+\varepsilon_G}\right)^{1.2}\left(\frac{\rho_L^2\rho_G}{\sigma^3}\right)^{0.2} \times\left(\frac{L_M}{d_M}\right)^{0.42}\left\{1-0.55\left(0.38-\frac{d_N}{d_M}\right)^2\right\} \quad (23)$$

For the *ejector with swirl device* used in this study, the flow transition point could be correlated as

$$\left(\frac{Q_G}{Q_L}\right)_{Trans} = C_8\left(\frac{d_N}{d_M}\right)\left(\frac{L_M}{d_M}\right)^{-0.38} \quad (24)$$

The k_La-data obtained in the bubble flow regime could be correlated as

$$k_La = C_6(\epsilon_{Dis})^{0.65}\varepsilon_G\left(\frac{1+0.2\varepsilon_G}{1+\varepsilon_G}\right)^{1.2}\left(\frac{\rho_L^2\rho_G}{\sigma^3}\right)^{0.2} \times\left(\frac{L_M}{d_M}\right)^{0.42}\left(\frac{d_N}{d_M}\right)^{0.65} \quad (25)$$

whereas the data in the jet-annular flow regime were correlated as

$$k_La = C_7(\epsilon_{Dis})^{0.65}(1-\varepsilon_G)\left(\frac{d_N}{d_M}\right)^{0.65} \quad (26)$$

The predicted values of the above mentioned design correlations are generally within 10% accuracy of the measured values. It has to be stressed that the predicted k_La-values are only valid for coalescing, non-viscous systems and for the geometrical ejector dimensions as used in this study.

7. Conclusions

From the present investigation, it can be concluded that the ejector configuration has a significant effect on the mass transfer characteristics of ejectors. It was shown that

1. For a constant volumetric mass transfer coefficient in the ejector section, both the power-input per unit ejector volume and the relative ejector dimensions are required for a proper scale-up of the ejector. These scale rules are valid for both ejector configurations, with or without a swirl device present in the upstream section of the nozzle or not. However, when using a swirl device, it has to be assured that in scaling-up the swirl-number is also kept constant. Otherwise, the flow transition point is affected by scale.
2. A swirl device in the upstream section of the nozzle influences both the volumetric mass transfer coefficient and the hydrodynamics (flow regime) in the ejector. Without a swirl device the highest k_La-values are obtained.
3. The mixing tube length influences the volumetric mass transfer rates. The k_La-values increase when longer mixing tubes are used.
4. When using a swirl device in the nozzle, the volumetric mass transfer coefficient of the ejector decreases when the nozzle to mixing tube diameter ratio is increased. When no swirl device is included, there seems to be an optimum d_N/d_M ratio of approximately 0.4.
5. In the bubble flow regime, the volumetric mass transfer coefficient increases when higher density gases are used. The results could be explained by using Levich's theory, i.e. when the gas density is increases, smaller bubbles are dispersed resulting in an increase of the k_La-value.

References

[1] M.Z. Zhu, J. Hannon, A. Green, Chem. Eng. Sci. 47 (1992) 2847–2852.

[2] P.H.M.R. Cramers, L.L. van Dierendonck, A.A.C.M. Beenackers, Chem. Eng. Sci. 47 (9-11) (1992) 2251–2256.
[3] P.H.M.R. Cramers, A.A.C.M. Beenackers, L.L. van Dierendonck, Chem. Eng. Sci. 47 (13/14) (1992) 3557–3564.
[4] C.A.M.C. Dirix, K. van der Wiele, Chem. Eng. Sci. 45 (8) (1990) 2333–2340.
[5] H.J. Henzler, VT (Verfahrenstechnik) 15 (1981) 738–749.
[6] X. Changfeng, L. Renjie, D. Gance, Chem. React. Eng. Technol. 7 (1991) 143–149.
[7] D.A. Lewis, J.F. Davidson, Trans. Inst. Chem. Eng. 60 (1982) 283–291.
[8] R.P. Hesketh, A.W. Etchells, T.W.F. Russel, AIChE J. 33 (4) (1987) 663–667.
[9] G.M. Evans, PhD-Thesis, University of Newcastle, NSW, 1990.
[10] R.V. Calabrese, T.P.K. Chang, P.T. Dang, AIChE J. 32 (1986) 657–666.
[11] P.H.M.R. Cramers, R.F. Duveen, A.A.C.M. Beenackers, L.L. van Dierendonck, in: Proceedings of the Symposium on Catalysis in Multiphase Reactors European, Lyon, France, 7–9 December 1994, Paper C-III-4.
[12] Y. Kawase, M. Moo-Young, Chem. Eng. J. 43 (1991) B19–B41.
[13] M. Palmer, M. Musketh, in: Proceedings of the Second International Conference on Multiple Phase Flow, Vol. 16, No. 4, 1984, pp. 327–333.
[14] P.H.M.R. Cramers, G. Leuteritz, L.L. van Dierendonck, A.A.C.M. Beenackers, Chem. Eng. J. 53 (1993) 67–73.